⌘ *Author's Choice*

THE JOURNAL OF BIOLOGICAL CHEMISTRY VOL. 283, NO. 43, pp. 28934–28943, October 24, 2008

A Parasite Cysteine Protease Is Key to Host Protein Degradation and Iron Acquisition*[S]

Received for publication, July 29, 2008 Published, JBC Papers in Press, August 13, 2008, DOI 10.1074/jbc.M805824200

Theresa C. O'Brien[‡], Zachary B. Mackey[‡], Richard D. Fetter[§], Youngchool Choe[§], Anthony J. O'Donoghue[§], Min Zhou[§], Charles S. Craik[§], Conor R. Caffrey[‡], and James H. McKerrow[‡1]

From the [‡]Department of Pathology and Sandler Center for Basic Research in Parasitic Diseases, and the [§]Department of Biochemistry and Biophysics, California Institute for Quantitative Biomedical Research (QB3), University of California, San Francisco, California 94158

Cysteine proteases of the Clan CA (papain) family are the predominant protease group in primitive invertebrates. Cysteine protease inhibitors arrest infection by the protozoan parasite, *Trypanosoma brucei*. RNA interference studies implicated a cathepsin B-like protease, tbcatB, as a key inhibitor target. Utilizing parasites in which one of the two alleles of *tbcatb* has been deleted, the key role of this protease in degradation of endocytosed host proteins is delineated. TbcatB deficiency results in a decreased growth rate and dysmorphism of the flagellar pocket and the subjacent endocytic compartment. Western blot and microscopic analysis indicate that deficiency in tbcatB results in accumulation of both host and parasite proteins, including the lysosomal marker p67. A critical function for parasitism is the degradation of host transferrin, which is necessary for iron acquisition. Substrate specificity analysis of recombinant tbcatB revealed the optimal peptide cleavage sequences for the enzyme and these were confirmed experimentally using FRET-based substrates. Degradation of transferrin was validated by SDS-PAGE and the specific cleavage sites identified by *N*-terminal sequencing. Because even a modest deficiency in tbcatB is lethal for the parasite, tbcatB is a logical target for the development of new anti-trypanosomal chemotherapy.

Proteases are ubiquitous enzymes that function in virtually all biological phenomena. Two of the major groups of proteases, Clan CA (papain-like) cysteine proteases and Clan SA (trypsin-like) serine proteases, underwent an evolutionary inversion whereby the more abundant cysteine proteases of primitive eukaryotes gave way to serine proteases with the evolution of arthropods (1) (merops.sanger.ac.uk/). Therefore, an analysis of the role of cysteine proteases in protozoa can provide insights into differential use and molecular evolution of this protease class.

Trypanosoma brucei is a protozoan parasite and the causative agent of human African trypanosomiasis, a fatal disease that is transmitted by the bite of the tsetse fly. Only four drugs are available to treat human African trypanosomiasis: two for the first stage of the disease when parasites proliferate in the blood (pentamidine and suramin) and two for the second stage when parasites have established infection in the cerebrospinal fluid (melarsoprol and eflornithine). These drugs cause serious side effects and are expensive to manufacture and administer (2). There is an obvious and urgent need to develop new chemotherapies to treat human African trypanosomiasis.

Two Clan CA cysteine proteases have been identified in *T. brucei*: rhodesain, which is cathepsin L-like and most abundant (3), and tbcatB, a cathepsin B-like enzyme (4). Treatment of parasites in culture with the nonspecific cysteine protease inhibitor, benzyloxycarbonyl-phenylalanyl-alanyl diazomethane (Z-Phe-Ala-CHN_2)[2] is lethal to cultured parasites at 10 μM (5). Parasites treated with this inhibitor exhibit altered cell morphology, are unable to undergo cytokinesis, and are defective in host protein degradation (5, 6). Knockdown of tbcatB expression by RNA interference (RNAi) is also lethal in *T. brucei*, causing phenotypic defects similar to those seen with the inhibitor (4). In contrast, knockdown of rhodesain expression produced no abnormal phenotype in cultured parasites (4). These results led to the hypothesis that whereas tbcatB is less abundant, it is, nonetheless, essential to *T. brucei* survival in culture and is a key target of the inhibitor. Furthermore, when RNAi targeting tbcatB is induced in a mouse model of *T. brucei* infection, mice are cured of their infection.[3]

One clue to the function of tbcatB comes from the observation that a host iron-transporting protein, transferrin, accumulates in Z-Phe-Ala-CHN_2-treated and tbcatB RNAi knockdown parasites (4, 5). Transferrin serves as the sole source of iron for

* This work was supported, in whole or in part, by National Institutes of Health Grant AI35707 from the NIAID Tropical Disease Research Unit. This work was also supported by a National Science Foundation Graduate Research Fellowship (to T. C. O.) and the Sandler Family Supporting Foundation. The costs of publication of this article were defrayed in part by the payment of page charges. This article must therefore be hereby marked "*advertisement*" in accordance with 18 U.S.C. Section 1734 solely to indicate this fact.

⌘ *Author's Choice*—Final version full access.

[S] The on-line version of this article (available at http://www.jbc.org) contains supplemental Table S1.

[1] To whom correspondence should be addressed: 1700 4th St., Box 2550, University of California, QB3, San Francisco, CA 94158-2550. Tel.: 415-476-2940; Fax: 415-502-8193; E-mail: jmck@cgl.ucsf.edu.

[2] The abbreviations used are: Z-Phe-Ala-CHN_2, benzyloxycarbonylphenylalanyl-alanyl diazomethane; RNAi, RNA interference; FR, flanking region; D-PBS, Dulbecco's phosphate-buffered saline; Z-FR-AMC, benzyloxycarbonyl-phenylalanyl-arginyl-7-amido-4-methyl coumarin; DTT, dithiothreitol; PS-SCL, positional scanning combinatorial synthetic combinatorial library; ACC, 7-amino-4-carbamoylmethylcoumarin; Tf-R, transferrin receptor; BSA, bovine serum albumin; MES, 4-morpholineethanesulfonic acid; BisTris, 2-[bis(2-hydroxyethyl)amino]-2-(hydroxymethyl)propane-1,3-diol.

[3] Abdulla, M. (2008) *PLoS Negl. Trop. Dis.*, in press.

T. brucei and is rapidly degraded in an endosomal or lysosomal compartment in the parasite (7). Thus, accumulation of transferrin implicates tbcatB in the process of iron acquisition and suggests that transferrin may be a natural substrate of the protease.

The RNAi studies showed only modest knockdown of tbcatB mRNA and protein, yet the phenotype was dramatic (4). Therefore, to validate the previous RNAi data and further our understanding of the functional role of tbcatB, we generated a single allele deletion strain of *T. brucei* and, together with the inducible-RNAi strain, analyzed the effects of tbcatB deficiency on cell morphology, protease localization, and the iron acquisition pathway. We also expressed recombinant tbcatB and analyzed its substrate specificity profile both for clues as to the identity of natural substrates and as a means to determine subsite characterization that will aid future inhibitor design.

EXPERIMENTAL PROCEDURES

Culturing of T. brucei—All bloodstream form strains of *T. brucei* were incubated in 5% carbon dioxide at 37 °C in HMI-9 medium containing 10% heat-inactivated fetal bovine serum (Omega Scientific), 10% Serum Plus (JRH Biosciences), 1× penicillin/streptomycin. The pZJMTbCB clones were cultured in media containing, 5.0 μg/ml hygromycin B and 2.5 μg/ml G418, as well as 2.5 μg/ml phleomycin as previously described (4). Induction of RNAi was carried out by adding tetracycline to a final concentration of 100 ng/ml.

Generation of tbcatb Single-allele Knock-out T. brucei Clones (tbcatb$^{+/-}$)—To generate the targeting vector, a cassette containing the phleomycin resistance marker flanked by the 5′- and 3′-flanking regions (FR) of the *tbcatb* gene was constructed. The following primers were used: 5′-FR forward primer, 5′-gcggccgccagaagctccactgcctcgcattg-3′; 5′-FR reverse primer, 5′-gatatccatgtgtcaccggatttggggtctgca-3′; 3′-FR forward primer, 5′-tctagataggttgcacatcgttaaacctagag-3′; 3′-FR reverse primer, 5′-gggcccacatccttatcccttccccgagggcg-3′. The cassette was cloned into the pCR2.1 vector (Invitrogen) at NotI and ApaI restriction endonuclease sites. For electroporation, 10^8 strain trypanosomes were pelleted by centrifugation, washed twice with 10 ml of cytomix (8), and finally resuspended in 0.5 ml of cytomix. One hundred micrograms of the targeting vector was linearized with NotI restriction endonuclease, precipitated with ethanol, and resuspended in 100 μl of cytomix. The parasites and DNA suspensions were mixed in a 4-mm electroporator cuvette and pulsed with 1.7 kV and 25 microfarads. After pulsing, the parasites were transferred to 24 ml of complete medium and incubated overnight at 37 °C with 5% carbon dioxide. Phleomycin was added to the medium to select for clones having the targeting vector integrated into the genome. Proper integration into the *tbcatb* locus was verified by PCR.

T. brucei Growth Assay—Trypanosomes were cultured at a density of 1×10^4 cells/ml and counted using a hemocytometer after 24, 48, and 72 h.

Immunofluorescence Microscopy—*T. brucei* were harvested by centrifugation at 4 °C, washed in cold Dulbecco's phosphate-buffered saline (D-PBS), and fixed in 4% paraformaldehyde/D-PBS for 1 h at 4 °C. All subsequent washes were carried out with excess D-PBS. Fixed cells were washed and applied to 25-mm round coverslips that had been coated with polylysine (0.1% w/v in water, Sigma) and allowed to settle for 20 min at room temperature. The cells were permeabilized in D-PBS containing 0.1% Triton X-100 (Sigma) for 10 min, washed, and blocked for 1 h with 1% bovine serum albumin (BSA) prepared in D-PBS. After blocking, cells were incubated in rabbit anti-p67 antiserum (a gift from J. D. Bangs) (9) (diluted 1:400 in 1% BSA/D-PBS) for 1 h, washed, incubated in Texas Red goat anti-rabbit IgG (Molecular Probes) (diluted 1:400 in 1% BSA/D-PBS) for 1 h, washed, and mounted on slides with Prolong Gold Antifade Reagent with 4,6-diamidino-2-phenylindole (Invitrogen). The cells were visualized on an AxioImager M1 microscope (Zeiss), equipped with an X-Cite 120 fluorescence illumination system (EXFP Life Sciences).

Transmission Electron Microscopy—Approximately 40 million *T. brucei* were harvested by centrifugation at 4 °C. Pelleted parasites were resuspended in 1 ml of media for high pressure freezing using either a Bal-Tec HPM 010 or Wohlwend HPF Compact 01 high-pressure freezer (University of California, Berkeley Electron Microscopy Laboratory). The parasites were processed for conventional EM by freeze substitution in 1% OsO_4, 0.1% uranyl acetate in acetone using a Leica AFS2 and embedded in Eponate 12 resin. Sections were cut with a Leica Ultracut E ultramicrotome using a diamond knife and picked up on Pioloform films on slot grids. Sections were stained with uranyl acetate and Sato's lead, and photographed using a Gatan 4k × 4k camera on an FEI Spirit transmission electron microscope operated at 120 kV.

Immunoelectron Microscopy—*T. brucei* samples for immuno-EM were prepared by high pressure freezing as indicated above, except freeze substitution was conducted in 0.2% glutaraldehyde, 0.1% uranyl acetate in acetone. Following substitution, the samples were infiltrated in LR White resin at 4 °C, and UV-polymerized at −20 °C using benzoin methyl ether as the UV catalyst in the LR White. Sections were picked up on carbon-coated Pioloform films on nickel grids. Sections were incubated with primary antibodies (rabbit anti-tbcatB (4) or rabbit anti-transferrin receptor (a gift from P. Borst) (10), both diluted 1:400) and 10 nm gold secondary antibodies (complete antibodies absorbed to gold) (British BioCell International, distributed by Ted Pella) diluted in 1% BSA, 0.1% Tween 20 in PBS. After labeling, the sections were fixed 5 min with 1% glutaraldehyde in phosphate-buffered saline, rinsed with distilled water, and stained with uranyl acetate followed by Sato's lead as indicated above. Control sections were immunostained using this protocol but with omission of the primary antibody. Sections were photographed as indicated above.

Cloning and Expression of TbcatB in Pichia pastoris—Methods for cloning and expression of tbcatB in *P. pastoris* have been described previously.[4] Briefly, the sequence encoding the tbcatB zymogen (pro and mature regions of the protease) was amplified from a cDNA vector that contained the entire open

[4] Mallari, J. P., Shelat, A., Kosinski, A., Caffrey, C. R., Connelly, M., Zhu, F., McKerrow, J. H., and Guy, R. K. (2008) Bioorg. Med. Chem. Lett. **18,** 2883–2885. Epub 2008 April 8

reading frame of tbcatB (4). The forward and reverse primers amplified genomic regions 5′-gagtaaacgccgccctcgttgct-3′ and 5′-cgccgtgttgggtgcaagagg-3′, respectively. The amplified DNA was purified and ligated into expression vector pPICZαB (Invitrogen) and subsequent transfection and expression techniques were modified from those given by the manufacturer as previously described (3).

Purification of Recombinant tbcatB—Following a 48-h induction, *P. pastoris* cultures were centrifuged at 3000 × *g* for 10 min and the resulting supernatant containing recombinant tbcatB was lyophilized. The crude lyophilized protein was resuspended in 10% of the original volume in 50 mM sodium citrate buffer (pH 5.5) and desalted using PD-10 columns (GE Healthcare/Amersham Biosciences) by equilibrating in the same buffer. The solution was loaded onto a Mono Q 5/50 anion exchange column using an Akta Purifier-900 chromatography system (both GE Healthcare/Amersham Biosciences). A 50 mM MES (pH 6.5) buffer was used for column equilibration, sample loading, and protein elution, with a flow rate of 1 ml/min. Protein was eluted with a linear gradient of 0 to 1 M sodium chloride concentration over 20 min. Fractions of 0.5 ml were collected and subsequently checked for purity by SDS-PAGE and activity by hydrolysis of the fluorogenic peptide substrate benzyloxycarbonyl-phenylalanyl-arginyl-7-amido-4-methyl coumarin (Z-FR-AMC) (Peptides International, Inc.) (see enzyme activity assay below).

Radiolabeling of Cysteine Protease Active Sites with ^{125}I-Labeled Inhibitors—Ten microliters of Mono Q fractions containing recombinant tbcatB were labeled with the cathepsin B-specific active site label ^{125}I-MB-074 (11) for 1 h at room temperature in buffer containing 5 mM dithiothreitol (DTT) and subjected to SDS-PAGE. Once the gels were dried, labeling was visualized by autoradiography.

Deglycosylation of Recombinant TbcatB—A New England Biolabs PNGase F kit was used for deglycosylation of Mono Q-purified recombinant tbcatB. Methods were followed as described in the instruction manual.

Protease Activity Assay—Protease activity was measured using the fluorogenic peptide substrate Z-FR-AMC, which is cleaved by the protease to release free 7-amino-4-methyl coumarin fluorogenic leaving group. Enzyme samples were preincubated for 10 min in sodium citrate buffer (50 mM, pH 5.5) containing 4 mM DTT, giving a total volume of 100 μl. Following the preincubation period, 100 μl of dilute substrate (20 μM, prepared in the same buffer) was added to the enzyme solution to give a final concentration of 10 μM Z-FR-AMC and a final volume of 200 μl. Hydrolysis was measured at 25 °C using an automated microtiter plate spectrofluorimeter (Molecular Devices Flex Station). Excitation and emission wavelengths were 355 and 460 nm, respectively. One unit of activity was defined as that releasing 1 μmol of AMC min^{-1}. To determine the Michaelis constant, K_m, a range of substrate concentrations from 0.14 to 300 μM was used and the value estimated using graphics software (Prism4, GraphPad).

pH Activity Profiling of Recombinant TbcatB—Mono Q-purified tbcatB was assayed for protease activity with Z-FR-AMC using 50 mM sodium citrate buffers that ranged in pH from 3 to 8, with 0.5 pH unit increments. Protease activity was assayed as described above. Initial velocities were taken and assays were performed in duplicate.

Protease Inhibitor Profiling—Mono Q-purified tbcatB was assayed for protease activity with Z-FR-AMC in the presence of various protease-class selective inhibitors. The inhibitors used were K11777 (*N*-methylpiperazine-Phe-homoPhe-vinylsulfonephenyl) (12), CA074 (*N*-(L-3-trans-propylcarbamoyloxirane-2-carbonyl)-L-isoleucyl-L-pro line) (13), phenylmethylsulfonyl fluoride, and E64 (*N*-[*N*-(l-3-*trans*-carboxyoxirane-2-carbonyl)-l-leucyl]-agmatine). Enzyme samples (in 10 μl volume) were preincubated with inhibitor for 5 min in 90 μl of sodium citrate buffer (50 mM, pH 5.5) containing 4 mM DTT to give a total volume of 100 μl. The inhibitor concentration range used was 0.01 to 10 μM. Following incubation, the substrate was added in the same buffer to give a final concentration of 10 μM Z-FR-AMC and final volume of 200 μl. Protease activity was assayed as described above.

Substrate Specificity Profiling and Substrate Screen—The P1–P4 substrate specificity profile for tbcatB was determined using a completely diverse positional scanning synthetic combinatorial library (PS-SCL) (14). The library contained substrates that are N-terminal acetylated and possessed 7-amino-4-carbamoyl-methylcoumarin (ACC) as the fluorogenic leaving group. The procedures used to screen the library were modified from those previously described (14). Crude lyophilized tbcatB was assayed at 25 °C in buffer containing 50 mM sodium citrate buffer (pH 5.5), 100 mM NaCl, 10 mM DTT, 1 mM EDTA, 0.01% Brij-35, and 1% Me_2SO (from the substrates). The concentration of tbcatB in the assays was ~10 nM. Assays were performed in triplicate.

To test the predictive capability of the substrate specificity profile obtained, authentic 7-amino-4-methyl coumarin (AMC) peptide substrates that were either "good" or "poor" matches to the profile were selected for screening in the protease activity assay described above. The range of substrate concentrations used was 3.5 to 300 μM. The substrates were: Z-FR-AMC (Peptides International, Inc.), Z-Arg-Arg-AMC (Z-RR-AMC) (Peptides International, Inc.), Z-Arg-Glu-Lys-Arg-AMC (Z-REKR-AMC) (Bachem), Ac-Ile-Glu-Pro-Asp-AMC (Ac-IEPD-AMC) (Bachem), Ac-Ala-Ser-Thr-Asp-AMC (Ac-ASTD-AMC) (Bachem), Z-Leu-Arg-Gly-Gly-AMC (Z-LRGG-AMC) (Bachem), H-Arg-Gln-Arg-Arg-AMC (H-RQRR-AMC) (Bachem), Ac-Lys-Gln-Lys-Leu-Arg-AMC (Ac-KQKLR-AMC) (AnaSpec, Inc.), and Z-Arg-Arg-Leu-Arg-AMC (Z-RRLR-AMC), which was custom synthesized by SynPep. Michaelis constants were estimated for each substrate as described above.

Human Serum and T. brucei Protein Database Search—A database of host serum proteins was created by searching the Protein Data Bank (PDB) (15), using the keyword "serum" and limiting the search to *"Homo sapiens"* proteins. The results of the search were downloaded in FASTA format. The database of serum proteins was then screened using the EMBOSS fuzzpro protein pattern program (16) for the amino acid motif: P4, Arg/Lys; P3, Arg/Lys; P2, *X;* P1, Arg/Lys.

T. brucei proteins were also screened for the presence of the optimal substrate motif preference of tbcatB. The screen was carried out using the "Search Using Quick Matrix Method" Database Search option on Scansite's website (scansite.mit.edu) (17). Once

the motif (P4, Arg/Lys; P3, Arg/Lys; P2, *X*; P1, Arg/Lys) was entered, the following parameters were selected: organism class, invertebrates; database, SWISS-PROT; and single species, *brucei*. No limits were set for other parameters in the program.

In Vitro Digestion of Transferrin by TbcatB—Bovine transferrin was obtained from Invitrogen. 10 nM tbcatB was assayed with 200 nM transferrin in 50 mM sodium citrate buffer (pH 5.5), 100 mM NaCl, 10 mM DTT, 1 mM EDTA. After 24 and 48 h incubation at 25 °C, digestive products were separated on a 10% BisTris gel, adsorbed onto polyvinylidene difluoride and stained with PageBlue (Fermentas). Cleavage products were excised and subjected to N-terminal sequencing (Molecular Structure Facility, University of California, Davis, CA). Three internally quenched fluorescent peptides derived from transferrin, MZ1 (K(Mca)KCACSNHEK(Dnp)), MZ2 (K(Mca)-EYVTALQNK(Dnp)), and MZ3 (K(Mca)SRKDKAT CK(Dnp)) were synthesized by Fmoc (*N*-(9-fluorenyl)methoxycarbonyl) chemistry on a Symphony Quartet (Protein Technologies). Fluorescent assays were performed as outlined previously except excitation and emission wavelengths were 328 and 393 nm, respectively.

Lysate Preparation for Two-dimensional PAGE—*T. brucei* strain 221 and *tbcatb*$^{+/-}$ were harvested by centrifugation, washed once in D-PBS, and resuspended at ~1 × 10^8 cells/ml in lysis buffer (50 mM sodium acetate, pH 5.5, 1 mM EDTA, 1% Triton X-100, 5 mM DTT, and 5 μl/ml Protease Inhibitor Mixture Set II (CalBiochem, stock solution contains 20 mM 4-(2-aminoethyl)benzenesulfonyl fluoride-hydrochloride, 1.7 mM bestatin, 200 μM E-64 protease inhibitor, 85 mM EDTA-disodium, and 2 mM pepstatin)) that had been supplemented with 0.1 unit/μl of DNase (RNase-free, Roche), 45 μM RNase A (Roche), and 30 mM $MgCl_2$. The lysates were incubated on ice for 20 min and then cleared by centrifugation at 16,000 × *g* for 50 min at 4 °C. The protein concentration of the cleared lysates was determined by Bradford assay (18). If not used immediately, lysates were stored at −80 °C. Equal amounts of each lysate (200 μg) were prepared for isoelectric focusing and two-dimensional gel electrophoresis using the ReadyPrep Two-dimensional Cleanup Kit (Bio-Rad). The subsequent procedures used for IEF and two-dimensional gel electrophoresis were carried out as described in the ReadyPrep Two-dimensional Starter Kit (Bio-Rad) instruction manual. Bio-Rad ReadyStrip IPG strips, pH 4–7, were used for IEF and 8–16% Criterion Ready Gels (Bio-Rad) were used for SDS-PAGE. Following SDS-PAGE, the gels were immediately transferred to polyvinylidene difluoride membrane (Millipore), using procedures described below.

Western Blots of Two-dimensional PAGE Gels—Two-dimensional gels that had been transferred to polyvinylidene difluoride membranes were blocked for 1 h (10 mM Tris, pH 7.4, 5% dry milk, and 0.1% BSA, w/v). After blocking, membranes were incubated with rabbit anti-transferrin antiserum (1:2500 dilution) (described above) for 1 h and washed 3 times for 10 min with TBST (10 mM Tris, pH 7.4, 150 mM NaCl, 0.4% Tween 20). After washing, membranes were incubated with horseradish peroxidase-conjugated donkey anti-rabbit IgG (1:5000 dilution) (GE Healthcare/Amersham Biosciences) for 1 h. The blots were washed three times for 10 min with TBST and twice for 10 min with TBS (TBST without 0.4% Tween 20). Finally, the blots were visualized by ECL (GE Healthcare/Amersham Biosciences).

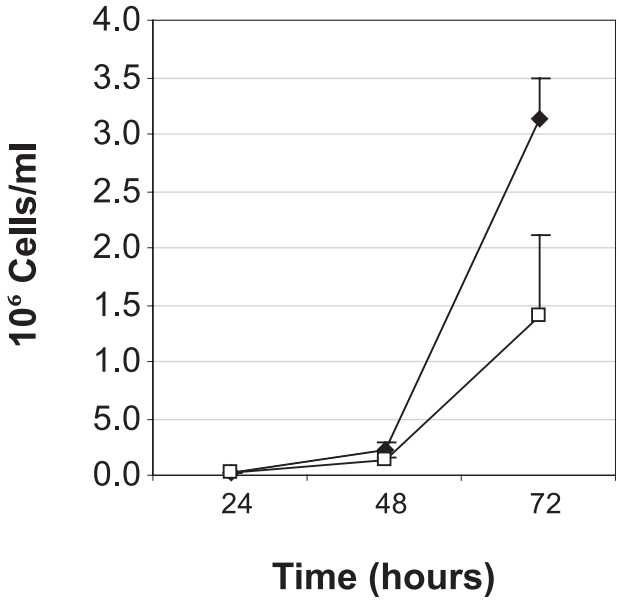

FIGURE 1. **Growth rate (replication) of 90-13 *versus* *tbcatb*$^{+/-}$ *T. brucei*.** One hundred thousand parasites were cultured at a density of 1 × 10^4 cells/ml and counted using a hemocytometer after 24, 48, and 72 h ($n = 3$). *Diamonds*, strain 90-13 (wild type); *open squares*, *tbcatb*$^{+/-}$.

Transferrin Starvation—Strain 221 and *tbcatb*$^{+/-}$ parasites were incubated at a density of 5 × 10^4 cells/ml for 36 h in appropriate media (see methods for culturing *T. brucei* above), containing 10% fetal bovine serum or, instead, dog serum (Innovative Research). After the incubation period, equal numbers of parasites (1 × 10^7) were resuspended in lysis buffer (50 mM sodium acetate, 1 mM EDTA, 1% Triton X-100, pH 5.5, 5 mM DTT). The lysates were incubated on ice for 20 min and cleared by centrifugation at 16,000 × *g* for 15 min at 4 °C. The extracts were resolved by SDS-PAGE and subjected to Western blot analysis, using procedures described above and rabbit anti-transferrin receptor antibody (a gift of P. Borst) (10) (diluted 1:250) as primary antibody. Labeling was quantified by densitometry using Image J software (National Institute of Health).

RESULTS

Single-allele Deletion of T. brucei Cathepsin B Gene Leads to Decreased Parasite Replication—Silencing of tbcatB by RNAi produced a marked phenotype (4). Parasites exhibited endosomal or lysosomal swelling, decreased growth rate, arrest in cytokinesis, and eventual death. However, this dramatic phenotype was associated with only a modest decrease in tbcatB mRNA, protein, and protease activity (4). Therefore, to validate and extend the RNAi results, a tbcatB heterozygous knock-out clone (*tbcatb*$^{+/-}$) was produced by homologous recombination using a *tbcatb* targeting vector. The rate of replication of the *tbcatb*$^{+/-}$ clones was ~40% less than the control 90-13 strain after 72 h (Fig. 1). *tbcatb*$^{-/-}$ clones could not be isolated due to presumed lethality.

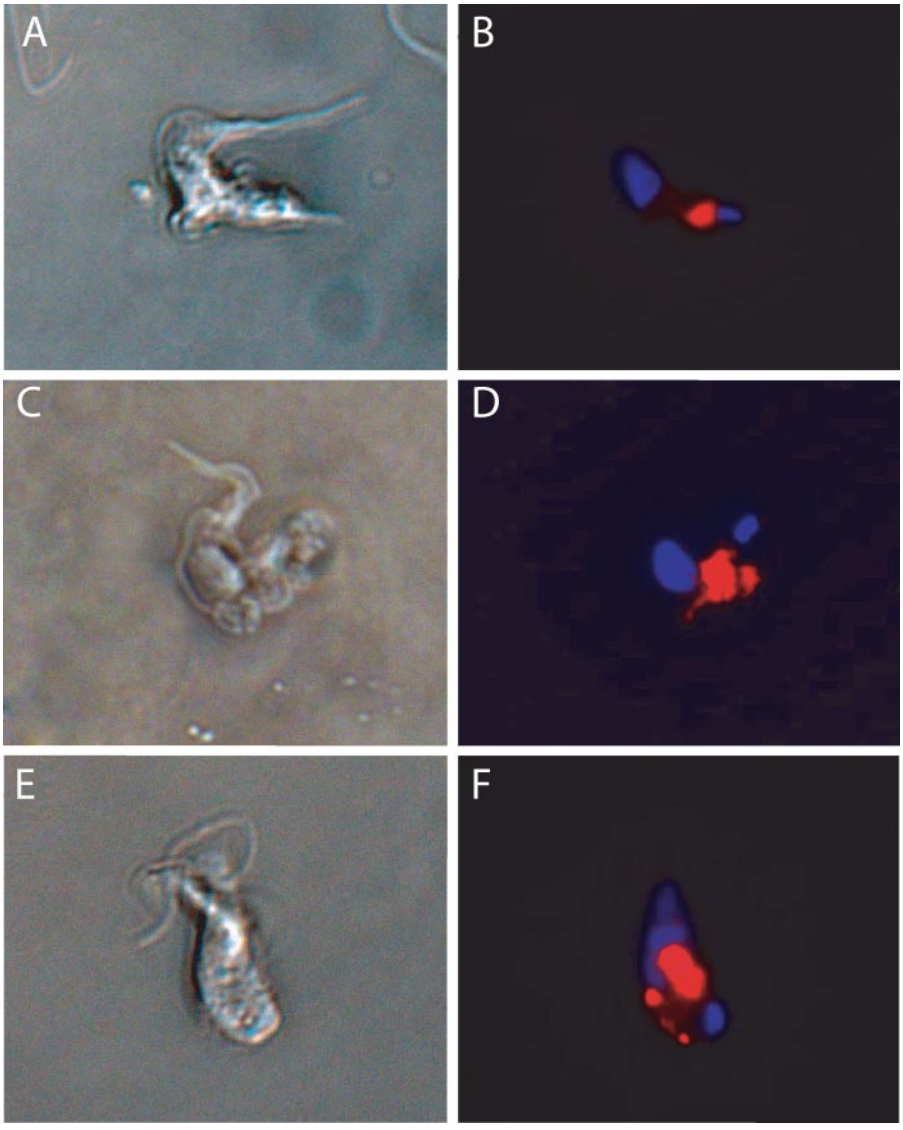

FIGURE 2. **Fluorescence localization of the lysosomal membrane glycoprotein p67 in pZJMTbCB and *tbcatb*$^{+/-}$clones.** *A, B, E,* and *F*, clones of pZJMTbCB were maintained as controls (*A* and *B*) or induced with tetracycline for 24 h (*E* and *F*). Cells were stained with rabbit anti-p67 antiserum and Texas Red goat anti-rabbit secondary antibody (*red channel*). 4,6-Diamidino-2-phenylindole was used to visualize DNA in the nucleus and kinetoplast by fluorescence microscopy (*blue channel*). *B* and *C*, *tbcatb*$^{+/-}$ clones (*B* and *C*) were prepared in an identical manner. Increased p67 labeling was observed in large, distorted organelles in *tbcatb*$^{+/-}$ clones (*D*) and parasites subjected to RNAi against tbcatB mRNA (*F*).

Abnormal Lysosomal and Flagellar Pocket Morphology in TbcatB-deficient Parasites—Treatment of wild-type *T. brucei* with the diazomethyl ketone cysteine protease inhibitor Z-Phe-Ala-CHN_2 lead to enlargement of the lysosome and an increase in total protein content, presumably as a result of decreased protein degradation (6). RNAi knockdown of tbcatB lead to similar lysosomal swelling (4). To compare the tbcatB-deficient phenotype with the phenotype of inhibitor-treated parasites, we first examined the lysosomal compartment by the localization of p67, a lysosomal type I membrane glycoprotein (19). In control parsasites, p67 staining was limited to a discrete organelle focus between the kinetoplast and nucleus (Fig. 2, *A* and *B*). In contrast, both induced RNAi clones (Fig. 2, *E* and *F*) and *tbcatb*$^{+/-}$ clones (Fig. 2, *C* and *D*) showed enhanced p67 labeling in large distorted organelles.

Electron microscopy was used to further delineate the phenotype of induced RNAi clones and *tbcatb*$^{+/-}$ parasites. In contrast to controls (Fig. 3, *A* and *B*), both the heterozygous knock-out (Fig. 3*C*) and RNAi knockdown (Fig. 3*D*) parasites had swollen flagellar pockets and swollen lysosomal compartments. The flagellar pockets of both tbcatB-deficient parasites were ~5 times larger in diameter than the flagellar pocket of the controls.

TbcatB Localizes to the Lysosome—Rhodesain, the most abundant cysteine protease activity in *T. brucei*, is found in the lysosome (3). Immunoelectron microscopy revealed that tbcatB, although less abundant, also localizes to lysosomes (Fig. 4*A*). When tbcatB expression is disrupted by RNAi, tbcatB protein fails to enter lysosomes but instead accumulates in adjacent tubular/vesicular structures (Fig. 4*B*), suggestive of an arrest in a post-Golgi vesicle.

Expression, Purification, and Biochemical Properties of Recombinant TbcatB from P. pastoris—Expression of the tbcatB zymogen lead to secretion of both zymogen and mature forms of tbcatB (42 and 31 kDa, respectively) from *P. pastoris* (Fig. 5*A*). The mature form was labeled by the cathepsin B-specific active site label ^{125}I-MB074 (11), indicating that the recombinant protease is indeed a cathepsin B-like enzyme (data not shown). We also observed ^{125}I-MB074 labeling with the zymogen because the label is small enough to access the active site even with the pro-domain intact (11). Purification of active tbcatB was carried out by lyophilization, desalting, and Mono Q anion exchange chromatography. Protease activity was monitored using the fluorogenic peptide substrate Z-FR-AMC. When the purified enzyme was subjected to deglycosylation with peptide:*N*-glycosidase F, a decrease in the molecular masses of both the zymogen and mature forms of the enzyme was observed: the zymogen and mature enzyme had increased mobility of ~8 and ~4 kDa, respectively, consistent with two glycosylation sites in the pro region (at amino acids Asn^{58}-Ile-Thr and Asn^{76}-Ala-Ser) and one in the mature region of tbcatB (Asn^{216}-Tyr-Thr). The optimal pH range for recombinant tbcatB with Z-FR-AMC was measured between pH 5.0 and 5.5 (Fig. 5*B*), consistent with the localization of the enzyme in an acidic

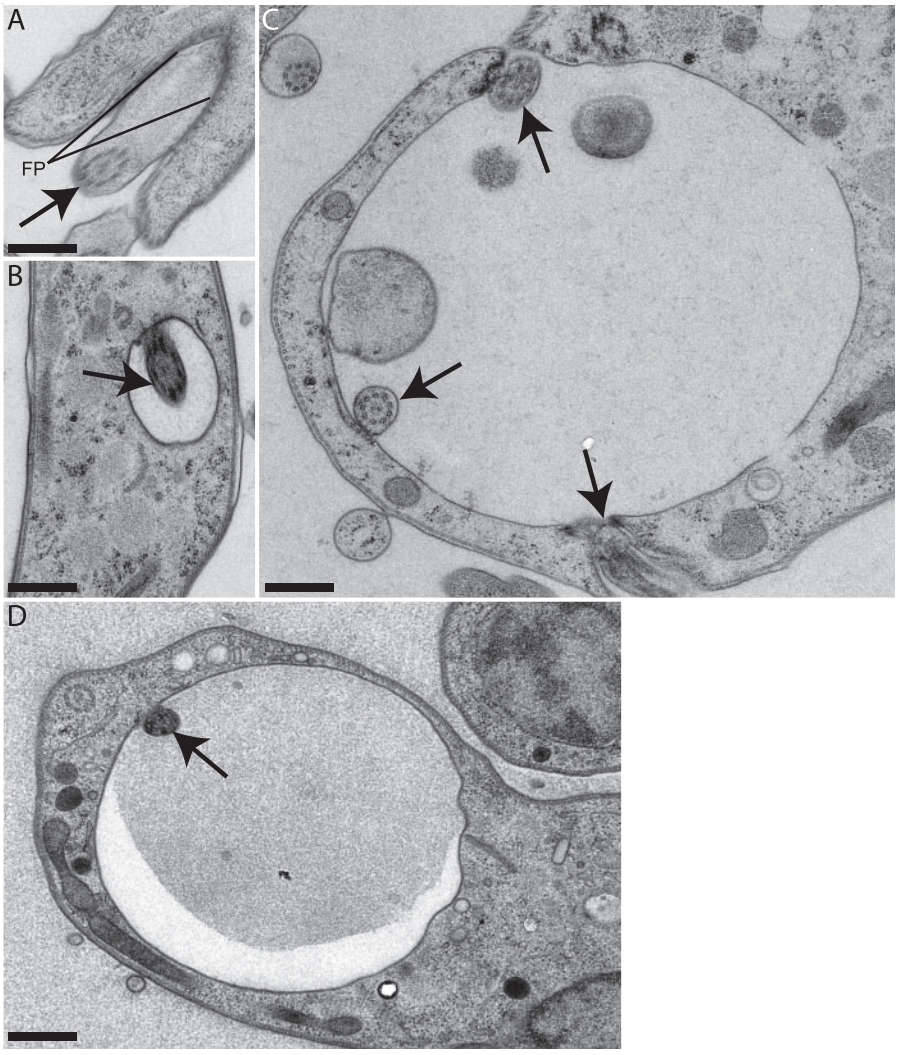

FIGURE 3. **Transmission electron microscopy of abnormal flagellar pocket and associated endocytic compartment morphology in pZJMTbCB and *tbcatb*$^{+/-}$ clones.** Clones of pZJMTbCB were maintained as controls (*A* and *B*) or induced with tetracycline for 24 h (*D*). Swollen flagellar pockets and lysosomes were observed in *tbcatb*$^{+/-}$ clones (*C*) and pZJMTbCB parasites induced with tetracycline (*D*). *Bar*, 0.5 μm. *Arrows* indicate flagellum (*A–C*) and multivesicular body at the edge of the lysosome (*D*). *FP* indicates the boundaries of the flagellar pocket in uninduced parasites.

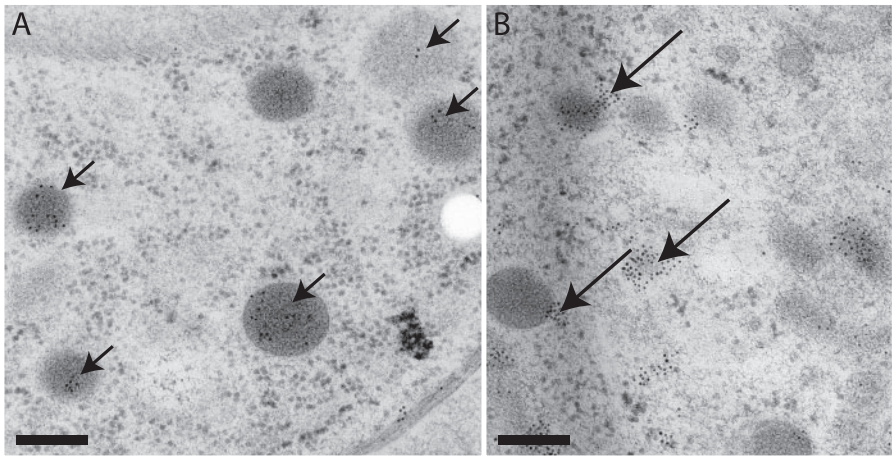

FIGURE 4. **Ultrathin cryosection immunogold labeling of tbcatB in strain 221 and pZJMTbCB parasites after RNA induction.** *A* and *B,* cross-sections were labeled with anti-tbcatB antiserum and 10-nm gold antibodies. Immunolabeling of tbcatB is observed in lysosomes in 221 parasites (*A*, *short arrows*) and outside, but proximal to, lysosomes in parasites subjected to RNAi against tbcatB mRNA (*B*, *long arrows*). *Bar*, 200 nm.

organelle. TbcatB activity was inhibited by the Clan CA cysteine protease inhibitors E-64 and K11777, but not by the serine protease inhibitor phenylmethylsulfonyl fluoride. The cathepsin B cysteine protease inhibitor, CA074, inhibited tbcatB better or as well as the generic clan CA cysteine protease inhibitors (E64 and K11777), confirming the cathepsin B-like activity of the recombinant enzyme.

Substrate Specificity Profiling of Recombinant TbcatB Identifies an Optimal Substrate Motif Preference—Substrate specificity profiling, using PS-SCLs, has been used to determine the P1–P4 preference of a protease for peptide substrates (20). Substrate specificity data obtained from screening a PS-SCL has facilitated natural substrate identification for S*chistosoma mansoni* legumain (21) and granzyme B (20, 22). Here, a complete diverse PS-SCL was used, containing 160,000 tetrapeptide substrates. This library completely randomizes each of the P1, P2, P3, and P4 positions with 20 amino acids (14). The PS-SCL demonstrated that tbcatB has a strong preference for arginine or lysine residues at P1 and for amino acids with large hydrophobic side chains at P2 (Fig. 6*A*). TbcatB was also more selective at P3 and P4 than its orthologs (14) (Fig. 6*B*) and P3 specificity differs significantly from that of human cathepsin B (Fig. 6*B*). The optimal substrate motif for tbcatB, as predicted by substrate specificity profiling, was: P4, Arg/Lys; P3, Arg/Lys; P2, *X;* P1, Arg/Lys.

The substrate specificity profile for tbcatB was verified by screening authentic fluorogenic peptide substrates that were predicted to be good or poor substrates for tbcatB. Only those substrates that most closely resembled the predicted optimal substrate motif for tbcatB were efficiently cleaved by the recombinant protease (Table 1).

Transferrin Is Degraded at Specific Sites by Recombinant tbcatB—A database of serum proteins was created to search for proteins that

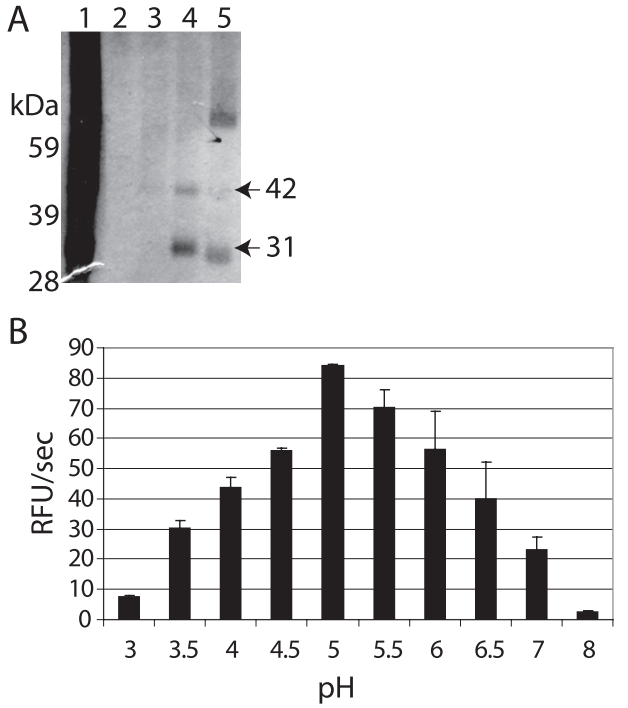

FIGURE 5. **Biochemical characterization and kinetic parameters of recombinant tbcatB.** *A*, recombinant tbcatB was expressed in *P. pastoris*. Crude protein was desalted, concentrated, and purified by anion exchange chromatography. Crude protein (*lane 1*), column flow-through (*lane 2*), and fractions (*lanes 3–5*) were resolved by SDS-PAGE and visualized by silver stain. Note both the zymogen at 42 kDa and more abundant mature form at 31 kDa (*lane 4*). *B*, pH-dependent activity of recombinant tbcatB. Protease was preincubated in 50 mM sodium citrate buffers (pH 3–8) containing 4 mM DTT. Then the same volume of respective buffer containing Z-FR-AMC was added. Activity was determined by hydrolysis of the substrate, measured by the fluorescence reporter AMC. *y* axis represents the rate of AMC production expressed as relative fluorescent units (*RFU*) per second. *x* axis represents the pH of the assay buffer.

contain a site that matched the predicted optimal substrate motif preference for tbcatB. The search identified 14 such proteins of which 9, including transferrin, contained a matching site that would be solvent accessible (see supplemental Table S1). A similar search was carried out for *T. brucei* proteins. Of note, a site matching the predicted optimal substrate motif preference in tbcatB was located in the propeptide of the rhodesain zymogen (KRLR, at amino acids 113–116) at the junction of the propeptide and mature domain.

To confirm degradation of native host transferrin, recombinant tbcatB was incubated with transferrin. After 24 h, 55- and 20-kDa products were identified by SDS-PAGE analysis. N-terminal sequence indicated that cleavage occurred between Ser^{203} and Asn^{204}. Secondary cleavage between Ala^{345} and Leu^{346} was evident after 48 h. As the primary and secondary cleavage sites in transferrin did not match the optimal predicted sequence, internally quenched fluorescent peptides encoding these sequences were synthesized and assayed with tbcatB. As expected, peptide MZ3 containing the RKDK site was the optimal substrate with a $k_{cat}/K_m = 2.5 \times 10^5$. Nevertheless, the actual primary and secondary cleavage sites identified in transferrin also gave reasonable k_{cat}/K_m values (1.3×10^5 for MZ1 the primary site and 9.3×10^3 for MZ2 the secondary site). This experiment confirms that tbcatB does indeed degrade transferrin, although at alternative sites than that predicted by the PS-SCL.

Undegraded Transferrin Accumulates in tbcatb$^{+/-}$ Parasites—Parasites internalize transferrin via receptor-mediated endocytosis in coated vesicles (23). These vesicles form at the flagellar pocket, the site of all endocytosis and excocytosis in *T. brucei*, and rapidly transit the endocytic system to the lysosome (reviewed in Ref. 24). Iron release is thought to occur in acidic vesicles, where transferrin is degraded in endosomal/lysosomal compartments and the transferrin receptor (Tf-R) is recycled to the flagellar pocket (7, 25). We examined the accumulation of transferrin in *tbcatb*$^{+/-}$ and control parasites by two-dimensional PAGE and Western blot analysis. Antibody to transferrin identified two protein species of ~64 and ~50 kDa in lysate obtained from *tbcatb*$^{+/-}$ parasites (Fig. 7*B*), whereas no transferrin species were detected in lysates obtained from wild-type parasites (Fig. 7*A*).

Tf-R Accumulation in TbcatB-deficient Parasites—*T. brucei* respond to low levels of intracellular iron by up-regulating the expression of the Tf-R (26). This up-regulation can alter the distribution of the receptor such that it accumulates in the flagellar pocket and on the surface

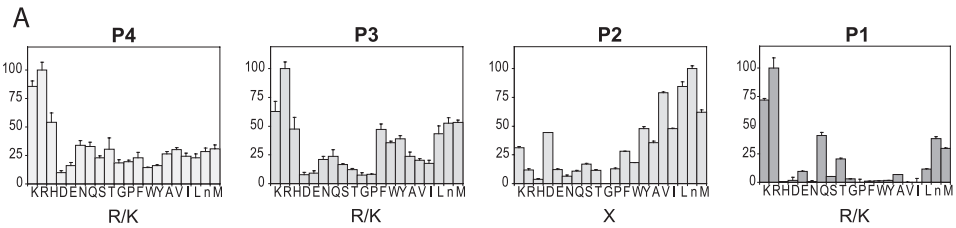

B

Preferred Substrate Motifs for Select Parasite and Human Cathepsins

	P4	P3	P2	P1
TbcatB	R/K	R/K	X	R/K
Papain	P/X	P/R	V	R/K
Cathepsin B	R/H/X	n/L	V/X	R/K
Cathepsin L	H/X	K/R/n	F/W/Y	R/K/Q
Rhodesain	H/X	R/P/K	F/W/L/Y	R/K
Cruzain	H/K/X	H/K/X	F/L/Y	R/K/Q

FIGURE 6. **Tetrapeptide substrate specificity profiling of tbcatB determined using complete diverse PS-SCL and comparison with related enzymes.** *A*, the library contained P1, P2, P3, and P4 libraries in which the P position is fixed with one of 20 amino acids (norleucine is used in place of isoleucine) and the other three positions are occupied by the 20 amino acids in an equimolar mixture. All of the substrates contained an ACC fluorogenic leaving group. Protease specificity was determined by hydrolysis of substrates, as measured by ACC fluorescence intensity. Assays were performed in triplicate and *error bars* denote the mean ± S.D. *y* axis represents the rate of ACC production expressed as a percentage of the maximum rate observed in each experiment. *x* axis indicates the amino acid held constant at position, designated by the one-letter code (with *n* representing norleucine), and amino acids are grouped along the axis to reflect the chemical properties of their side chains (acidic, basic, polar, aromatic, and aliphatic amino acids). *B*, a comparison of preferred substrate motifs for recombinant tbcatB, papain (14), human cathepsin B (14), human cathepsin L (14), rhodesain (14), and cruzain (14) determined using the complete diverse library.

TABLE 1

Kinetic analysis of fluorescent peptide substrates with recombinant tbcatB

To test the predictive power of the substrate specificity profile obtained for tbcatB, di-, tetra-, and pentapeptide substrates that were either good or poor matches to the profile were selected for screening. All substrates contained an AMC fluorogenic leaving group and assays were carried out in duplicate. Kinetic parameters are shown for eight commercially obtained substrates: Z-FR, Z-RR, Ac-KQKLR, Z-RRLR, Z-REKR, Ac-ASTD, H-RQRR, Ac-IEPD, Z-LRGG, and Z-RRLR (synthesized by Synpep). Amino acid sequence is indicated using single-letter code. Note that K_m and k_{cat} values for Ac-IEPD and Z-LGRR could not be measured (indicated as NM in the table), as they demonstrated poor binding and poor turnover. A K_m value could not be measured for Ac-ASTD, although the substrate did have a low k_{cat}.

AMC substrate	k_{cat}	K_m	k_{cat}/K_m	Class
	$s^{-1} \times 10^{-2}$	μM	$M^{-1} s^{-1}$	
Z-RRLR	10 ± 0.5	15.4 ± 3.0	6.50×10^4	Good
Z-FR	4.5 ± 0.5	19.2 ± 8.3	2.34×10^4	Good
Ac-KQKLR	10.9 ± 0.2	53.4 ± 3.0	2.05×10^4	Good
Z-RR	4.8 ± 0.2	68.7 ± 8.3	0.70×10^4	Good
Z-REKR	0.6 ± 0.0	35.6 ± 7.7	0.16×10^4	
H-RQRR	0.2 ± 0.0	19.2 ± 8.7	0.09×10^4	
Ac-ASTD	0.3 ± 0.1	NM[a]	NM	Poor
Ac-IEPD	NM	NM	NM	Poor
Z-LRGG	NM	NM	NM	Poor

[a] NM, not measured.

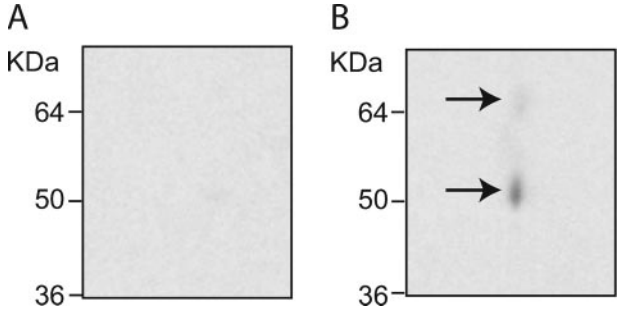

FIGURE 7. **Transferrin accumulation in stain 221 and *tbcatb*$^{+/-}$ *T. brucei*.** Parasites were harvested, lysed, and protein concentration of the lysates was determined by Bradford assay. Two hundred micrograms of 221 and *tbcatb*$^{+/-}$ lysates was prepared using the ReadyPrep Two-dimensional Cleanup Kit (Bio-Rad), which removes ionic detergents, salts, nucleic acids, lipids, and other substances. Lysates were subjected to isoelectric focusing and finally resolved by SDS-PAGE. Transferrin was visualized by Western blot analysis using anti-transferrin antiserum and horseradish peroxidase-conjugated donkey anti-rabbit IgG. Antibody staining was observed only in the *tbcatb*$^{+/-}$ blot (*B*, *arrows*); no signal was observed in the 221 blot (*A*).

of the parasite (10). Additionally, iron-starved parasites can switch transferrin receptors, exchanging the Tf-R expression site to one that expresses a receptor with higher affinity for host transferrin (27, 28).

To explore the hypothesis that tbcatB-deficient parasites undergo iron starvation due to lack of transferrin degradation, we examined the expression and localization of the Tf-R in tbcatB heterozygous knockouts and tbcatB RNAi knockdowns, respectively. Up-regulation of Tf-R expression was first confirmed using an iron-starvation assay in which parasites were cultured in media containing 10% dog serum *versus* the fetal calf serum that is typically used. The *T. brucei* transferrin receptor expressed by strain 221 parasites has a very low affinity for dog serum transferrin (28) and the parasites respond by up-regulating Tf-R expression (26). In *tbcatb*$^{+/-}$ parasites, the Tf-R is up-regulated by more than 40% above the wild type strain, suggesting that the tbcatB-deficient parasites experience a severe starvation phenotype (Fig. 8, *A* and *B*). Tetracycline-induced pZJMTbCB parasites accumulated abundant Tf-R in swollen flagellar pockets (Fig. 8*C*), whereas controls did not (Fig. 8*D*).

DISCUSSION

Both *in vitro* and *in vivo* studies have shown that cysteine protease activity is required for *T. brucei* survival (5, 6, 29, 30). RNAi studies implicated tbcatB as an essential protease (4).[3] However, only modest loss of tbcatB RNA and protease activity is achieved with RNAi (4). Therefore, to validate these results, we now show that parasites containing only a single copy of the tbcatB gene (*tbcatb*$^{+/-}$ clones) exhibit decreased growth rate and morphological abnormalities similar to those observed in studies using cysteine protease inhibitors (5, 6, 29) or RNAi knockdown of tbcatB (4).

The abnormalities in *T. brucei* organelle morphology produced by cysteine protease inhibitors led to the hypothesis that cysteine proteases are required to degrade host proteins (5, 6). Parasites treated with Z-Phe-Ala-CHN_2 had an enlargement of the lysosome (5, 6). A similar enlargement of the lysosomal/endosomal compartment was observed with tbcatB RNAi knockdown parasites (4) and the same abnormality is seen in *tbcatb*$^{+/-}$ parasites (Fig. 2). Using antibody localization of p67, accumulation of this specific lysosomal protein in an enlarged, dysmorphic organelle was confirmed. The compartmental swelling seen in Fig. 3 also includes the flagellar pocket. The bulk of host proteins taken up by trypanosomes first enter the flagellar pocket and are subsequently trafficked to the lysosome. Therefore, the accumulation of undegraded proteins and the presumed osmotic consequences might be expected to affect not only the lysosome, but also the endosomal and flagellar pocket compartments. This is what is observed in Fig. 3, as well as in a previous study, following deletion of a cassette of cysteine proteases in the related kinetoplastid parasite, *Leishmania mexicana* (31, 32). A similar phenotype was also noted in parasites in which RNAi targeted Rab5 (33), Rab11 (34), actin (35), or clathrin (36) transcripts, all coding for key proteins required for endocytosis.

Results of cysteine protease inhibitor studies suggest a key role for *T. brucei* cysteine proteases in host protein degradation (5, 6, 29). Specifically, host transferrin is a likely substrate as protease inhibitor-treated parasites accumulated fluorescently labeled transferrin (5). Subsequent RNAi studies revealed that knockdown of tbcatB also resulted in an accumulation of transferrin (4). In this study, we have used a positional scanning library to identify optimal substrates for tbcatB. Using this data, a predicted cleavage site was identified in transferrin. *In vitro* studies confirmed that transferrin is digested by tbcatB, however, N-terminal sequencing indicated that cleavage occurs at two exposed sites on the surface of the protein that differ from the predicted site. Peptides encoding the predicted and actual cleavage sites were digested and kinetic studies determined that the predicted site is not accessible to tbcatB.

With the generation of tbcatB heterozygous knock-out parasites, we have confirmed that transferrin accumulates in parasites as a result of tbcatB deficiency. Accumulation of Tf-R within the flagellar pocket of tbcatB knockdowns, and

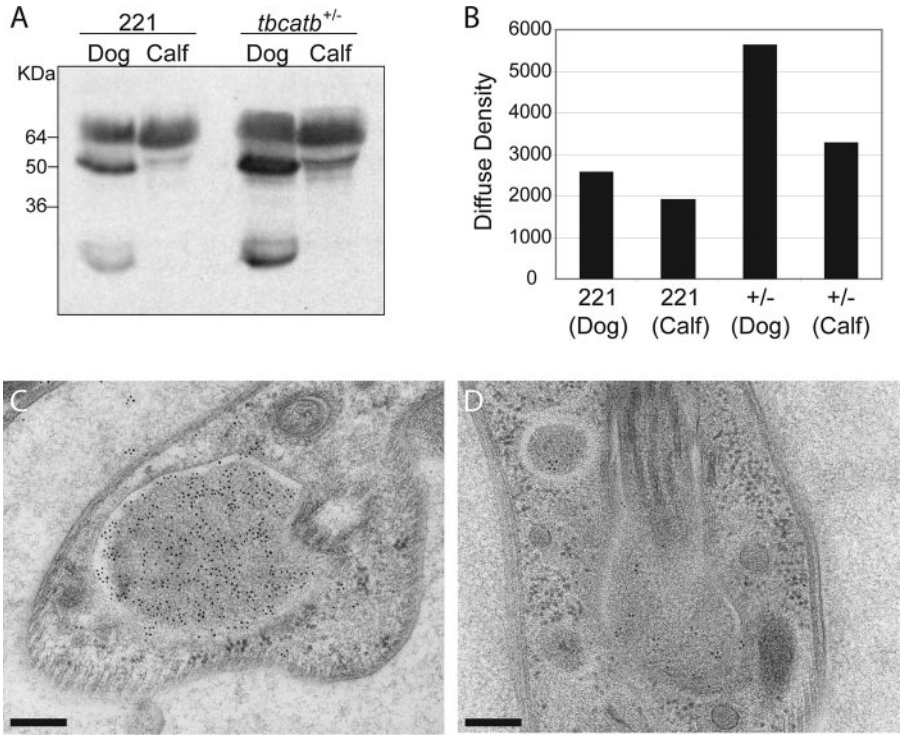

FIGURE 8. **Accumulation of transferrin receptor in pZJMTbCB clones after RNAi induction and in *tbcatb*$^{+/-}$ parasites.** *A* and *B,* strain 221 and *tbcatb*$^{+/-}$ parasites were incubated for 36 h in media containing either dog serum (*Dog*) or fetal calf serum (*Calf*) at a density of 5×10^4 cells/ml. Media for *tbcatb*$^{+/-}$ parasites was supplemented with 2.5 μg/ml phleomycin. After the incubation period, equal numbers of parasites were lysed and the extract resolved by SDS-PAGE for Western blot analysis with transferrin receptor antiserum (*A*). Labeling was quantified for each lane by densitometry (*B*). Transferrin receptor antibody labeling (70 and 52 kDa bands) is greater in dog serum samples when compared with fetal calf serum samples, and greater in *tbcatb*$^{+/-}$ extracts when compared with 221 extracts. *C* and *D*, thin sections from samples of strain 221 parasites and pZJMTbCB clones that had been induced with tetracycline for 24 h and prepared by high pressure freezing and freeze substitution. The sections were labeled with anti-transferrin receptor antiserum and 10-nm gold antibodies. Immunolabeling of transferrin receptor was observed in the swollen flagellar pockets of the RNAi-induced parasites (*C*) but not in controls (*D*). *Bar*, 200 nm.

up-regulation of Tf-R protein levels in tbcatB-deficient parasites, are both responses to iron starvation (26). The observation that both abnormalities occur in *tbcatb*$^{+/-}$ parasites supports the hypothesis that tbcatB is required for proper acquisition of iron.

Although iron starvation is an important physiologic defect in tbcatB deficiency, other host and parasite proteins are likely substrates for this enzyme in the endosome/lysosome of the parasite. The lysosomal protein, p67, is a potential substrate. This is consistent with the previous observation that a broad-spectrum cysteine protease inhibitor, leupeptin, inhibited p67 processing (37, 38). Two other parasite proteins were also identified as enriched (undegraded) in two-dimensional gel electrophoresis of parasite lysates following RNAi treatment, or in *tbcatb*$^{+/-}$ parasite lysates (data not shown). These were the zymogen of the cathepsin L protease, rhodesain, and the variant surface glycoprotein. However, accumulation of both of these proteins was only seen in parasites where lysates were made in the absence of SDS. These parasite lysates might still contain active proteases, so processing of the two parasite proteins may have occurred following the preparation of the lysates rather than *in situ*. Nevertheless, these results suggest that if tbcatB encounters either of these proteins during the lifecycle of *T. brucei*, they are potential substrates. Indeed, rhodesain has been localized to the lysosome (3) and some variant surface glycoprotein may be turned over in that compartment (39). Furthermore, the identification of a preferred cleavage motif for tbcatB by PS-SCL adjacent to the activation site of pro-rhodesain, raises the intriguing possibility that tbcatB may be responsible for activation of the abundant rhodesain protease in the lysosome or a pre-lysosome compartment.

In summary, *T. brucei* cathepsin B-like protease is a key enzyme in host protein turnover and iron acquisition in *T. brucei* parasites. Even a modest reduction of this enzyme by RNAi induction leads to organelle dysmorphism and parasite death (4). The present study utilizing parasites in which a single allele of the *tbcatB* gene is deleted validates RNAi studies, suggesting that the physiologic concentration of tbcatB is at a critical level, where even modest reduction can have a profound effect on the parasite. The drugability of parasite Clan CA cysteine protease inhibitors is well established (12, 40, 41) and the present report suggests that *T. brucei* cathepsin B is a logical target for the development of new anti-trypanosomal chemotherapy.

Acknowledgments—We thank George A. M. Cross (The Rockefeller University, New York, NY) for the T. brucei 90-13 strain, Paul T. Englund (Johns Hopkins Medical School, Baltimore, MD) for the pZJM and pLew111 vectors, Matt Bogyo for the ^{125}*I-MB074 active site probe (Stanford University, Stanford, CA), James D. Bangs (University of Wisconsin School of Medicine and Public Health, Madison, WI) for the anti-p67 antiserum, Piet Borst (The Netherlands Cancer Institute, Amsterdam, The Netherlands) for the anti-transferrin receptor antiserum, and Kent McDonald at the University of California Berkeley Electron Microscopy Lab for access to the high pressure freezing devices. We also thank Elizabeth Hansell, Christopher Franklin, Juan Engel, and Susan Jean Johns for technical assistance and Mohammed Sajid for editorial comments.*

REFERENCES

1. Rawlings, N. D., Tolle, D. P., and Barrett, A. J. (2004) *Nucleic Acids Res.* **32,** D160–D164
2. Luscher, A., de Koning, H. P., and Maser, P. (2007) *Curr. Pharm. Des.* **13,** 555–567
3. Caffrey, C. R., Hansell, E., Lucas, K. D., Brinen, L. S., Alvarez Hernandez, A., Cheng, J., Gwaltney, S. L., 2nd, Roush, W. R., Stierhof, Y. D., Bogyo, M.,

Steverding, D., and McKerrow, J. H. (2001) *Mol. Biochem. Parasitol.* **118,** 61–73
4. Mackey, Z. B., O'Brien, T. C., Greenbaum, D. C., Blank, R. B., and McKerrow, J. H. (2004) *J. Biol. Chem.* **279,** 48426–48433
5. Scory, S., Caffrey, C. R., Stierhof, Y. D., Ruppel, A., and Steverding, D. (1999) *Exp. Parasitol.* **91,** 327–333
6. Scory, S., Stierhof, Y. D., Caffrey, C. R., and Steverding, D. (2007) *Kinetoplastid. Biol. Dis.* **6,** 1–6
7. Steverding, D. (2000) *Parasitol. Int.* **48,** 191–198
8. van den Hoff, M. J., Christoffels, V. M., Labruyere, W. T., Moorman, A. F., and Lamers, W. H. (1995) *Methods Mol. Biol.* **48,** 185–197
9. Kelley, R. J., Alexander, D. L., Cowan, C., Balber, A. E., and Bangs, J. D. (1999) *Mol. Biochem. Parasitol.* **98,** 17–28
10. Mussmann, R., Janssen, H., Calafat, J., Engstler, M., Ansorge, I., Clayton, C., and Borst, P. (2003) *Mol. Microbiol.* **47,** 23–35
11. Bogyo, M., Verhelst, S., Bellingard-Dubouchaud, V., Toba, S., and Greenbaum, D. (2000) *Chem. Biol.* **7,** 27–38
12. Engel, J. C., Doyle, P. S., Hsieh, I., and McKerrow, J. H. (1998) *J. Exp. Med.* **188,** 725–734
13. Buttle, D. J., Murata, M., Knight, C. G., and Barrett, A. J. (1992) *Arch. Biochem. Biophys.* **299,** 377–380
14. Choe, Y., Leonetti, F., Greenbaum, D. C., Lecaille, F., Bogyo, M., Bromme, D., Ellman, J. A., and Craik, C. S. (2006) *J. Biol. Chem.* **281,** 12824–12832
15. Berman, H. M., Westbrook, J., Feng, Z., Gilliland, G., Bhat, T. N., Weissig, H., Shindyalov, I. N., and Bourne, P. E. (2000) *Nucleic Acids Res.* **28,** 235–242
16. Rice, P., Longden, I., and Bleasby, A. (2000) *Trends Genet* **16,** 276–277
17. Obenauer, J. C., Cantley, L. C., and Yaffe, M. B. (2003) *Nucleic Acids Res.* **31,** 3635–3641
18. Bradford, M. M. (1976) *Anal. Biochem.* **72,** 248–254
19. Alexander, D. L., Schwartz, K. J., Balber, A. E., and Bangs, J. D. (2002) *J. Cell Sci.* **115,** 3253–3263
20. Loeb, C. R., Harris, J. L., and Craik, C. S. (2006) *J. Biol. Chem.* **281,** 28326–28335
21. Mathieu, M. A., Bogyo, M., Caffrey, C. R., Choe, Y., Lee, J., Chapman, H., Sajid, M., Craik, C. S., and McKerrow, J. H. (2002) *Mol. Biochem. Parasitol.* **121,** 99–105
22. Harris, J. L., Peterson, E. P., Hudig, D., Thornberry, N. A., and Craik, C. S. (1998) *J. Biol. Chem.* **273,** 27364–27373
23. Grab, D. J., Shaw, M. K., Wells, C. W., Verjee, Y., Russo, D. C., Webster, P., Naessens, J., and Fish, W. R. (1993) *Eur. J. Cell Biol.* **62,** 114–126
24. Pal, A., Hall, B. S., Jeffries, T. R., and Field, M. C. (2003) *Biochem. J.* **374,** 443–451
25. Kabiri, M., and Steverding, D. (2000) *Eur. J. Biochem.* **267,** 3309–3314
26. Mussmann, R., Engstler, M., Gerrits, H., Kieft, R., Toaldo, C. B., Onderwater, J., Koerten, H., van Luenen, H. G., and Borst, P. (2004) *J. Biol. Chem.* **279,** 40690–40698
27. van Luenen, H. G., Kieft, R., Mussmann, R., Engstler, M., ter Riet, B., and Borst, P. (2005) *Mol. Microbiol.* **58,** 151–165
28. Gerrits, H., Mussmann, R., Bitter, W., Kieft, R., and Borst, P. (2002) *Mol. Biochem. Parasitol.* **119,** 237–247
29. Nkemgu, N. J., Grande, R., Hansell, E., McKerrow, J. H., Caffrey, C. R., and Steverding, D. (2003) *Int. J. Antimicrob. Agents* **22,** 155–159
30. Caffrey, C. R., Scory, S., and Steverding, D. (2000) *Curr. Drug. Targets* **1,** 155–162
31. Brooks, D. R., Tetley, L., Coombs, G. H., and Mottram, J. C. (2000) *J. Cell Sci.* **113,** 4035–4041
32. Mottram, J. C., Frame, M. J., Brooks, D. R., Tetley, L., Hutchison, J. E., Souza, A. E., and Coombs, G. H. (1997) *J. Biol. Chem.* **272,** 14285–14293
33. Hall, B., Allen, C. L., Goulding, D., and Field, M. C. (2004) *Mol. Biochem. Parasitol.* **138,** 67–77
34. Hall, B. S., Smith, E., Langer, W., Jacobs, L. A., Goulding, D., and Field, M. C. (2005) *Eukaryot. Cell* **4,** 971–980
35. Garcia-Salcedo, J. A., Perez-Morga, D., Gijon, P., Dilbeck, V., Pays, E., and Nolan, D. P. (2004) *EMBO J.* **23,** 780–789
36. Allen, C. L., Goulding, D., and Field, M. C. (2003) *EMBO J.* **22,** 4991–5002
37. Brickman, M. J., and Balber, A. E. (1994) *J. Cell Sci.* **107,** 3191–3200
38. Kelley, R. J., Brickman, M. J., and Balber, A. E. (1995) *Mol. Biochem. Parasitol.* **74,** 167–178
39. Triggs, V. P., and Bangs, J. D. (2003) *Eukaryot. Cell* **2,** 76–83
40. Doyle, P. S., Zhou, Y. M., Engel, J. C., and McKerrow, J. H. (2007) *Antimicrob. Agents Chemother.* **51,** 3932–3939
41. Renslo, A. R., and McKerrow, J. H. (2006) *Nat. Chem. Biol.* **2,** 701–710